

A mathematical model for pulsatile flow of Herschel-Bulkley fluid through stenosed arteries

S. U. Siddiqui, N. K. Verma and R. S. Gupta *

Department of Mathematics, Harcourt Butler Technological Institute, Kanpur, India

*Department of Mathematics, Kamla Nehru Institute of Technology, Sultanpur, India

Abstract. Presented herein is the study of pulsatile flow of blood through stenosed artery by modeling blood as Herschel–Bulkley fluid. The Herschel–Bulkley fluid has two parameters, the yield stress θ and the power index n . Perturbation method is used to solve the resulting quasi-steady nonlinear coupled implicit system of differential equations. The effects of pulsatility and non-Newtonian nature of blood on velocity, flow rate, wall shear stress and longitudinal impedance of the artery are discussed. The width of the plug core region increases with increasing value of yield stress at any time. The velocity and flow rate decrease, whereas wall shear stress and longitudinal impedance increase for increasing value of yield stress with other parameters held fixed. On the other hand, the velocity, flow rate and wall shear stress decrease but resistance to flow increases as the radius of artery increases with other parameters fixed. The results for power law fluid, Newtonian fluid and Bingham fluid are obtained as special cases from this model.

Keywords. Pulsatile blood flow; Stenosed artery; Herschel–Bulkley fluid; Yield stress; Wall shear stress; Longitudinal impedance.

Introduction

Diseases of the heart and circulatory system are still a major cause of death in the industrialized world. Blood flow characteristics in arteries can be altered significantly by arterial disease, such as stenosis and aneurysm. The altered haemodynamics may further influence the development of the disease and arterial deformity, and change the regional blood rheology [23] (Smedby, 1997). The study of physiologically realistic pulsatile through stenosis has profound implications for the diagnosis and treatment of vascular disease. The possibility that hemodynamic factors may participate in the genesis and proliferation of atherosclerosis has fostered increased study of flow through constrictions during the past decade [2,9] (Despande et al., 1976; Back et al., 1986). Realizing the fact that the pulsatile nature of the flow cannot be neglected, many theoretical analysis and experimental studies of the flow through stenosis have been performed [5,15,17,19,20]. In 1987, Haldar [11] dealt with the problem of oscillatory blood flow through a rigid tube with mild constriction under a simple harmonic pressure gradient and has examined the effect of stenosis on the flow field. In most of the studies mentioned above, the flowing blood is assumed to be Newtonian. The assumption of the Newtonian behaviour of blood is acceptable for a high shear rate flow in the case of a flow through larger arteries. It has now been well accepted that blood, being suspension of cells, behaves like a non-Newtonian fluid at allow shear rate in smaller arteries under certain flow conditions [4,10,13,14,18]. In 2004, Chakravarty et.al. [4] presented a theoretical investigation to examine some of the significant characteristics of the two-layered non-Newtonian rheology of blood

flowing through a tapered flexible artery in the presence of stenosis under a pulsatile pressure gradient. The papers [6,7,8,21,26] provide a small sample of the research in non-Newtonian effects on blood flow. A less-studied area is the usage of numerical optimization procedures to guide the design process that involves blood flow. It is, therefore of interest to consider simultaneously the effects of pulsatility, stenosis, and non-Newtonian behaviour of blood on its flow.

Aroesty and Gross [1] have studied the pulsatile flow of blood in small blood vessels and Chaturani and Ponnalagar Samy [6] extended this theory to study pulsatile flow of blood in stenosed arteries, modeling blood by Casson fluid. Scott Blair and Spanner [21] reported that blood obeys Casson equation only for moderate shear rate and that there is no difference between Casson's and Herschel–Bulkley's plot over the range where Casson's plot is valid for blood. It has been reported by Tu and Deville [24] that the assumption of Newtonian behaviour of blood is acceptable for high shear rate flow, e.g. in the case of flow through large arteries. It has also been pointed out that in some diseased conditions, e.g. patients with severe myocardial infarction, cerebrovascular diseases and hypertension, blood exhibits remarkable non-Newtonian properties [13]. It is true that the Casson fluid model can be used for moderate shear rates $\dot{\gamma} < 10 \text{ s}^{-1}$ in smaller diameter tubes whereas, the Herschel–Bulkley fluid model can be used at still lower shear rate of flow in very narrow arteries where the yield stress is high [17] and [19]. Also Herschel–Bulkley fluid model can be reduced to that of power law, Bingham and Newtonian fluid models by suitable choice of the parameters. The same model can be used for larger arteries where the effect of yield stress can be ignored. Hence it is appropriate to model blood as a Herschel–Bulkley fluid rather than Casson fluid.

In this paper, an attempt has been made to study the effects pulsatility and non-Newtonian nature of blood on physiologically important flow quantities such as velocity, flow resistance and wall shear stress for blood flow in an artery by modeling blood as Herschel–Bulkley fluid. The physical quantities involved in the problem are non-dimensionalized and the expressions for flow quantities such as velocity, flow rate, wall shear stress and longitudinal impedance of the artery are obtained for pulsatile flow. The effects of pulsatility, generalized Womersley frequency parameter and yield stress of the fluid on velocity profiles, flow rate, wall shear stress and longitudinal impedance are analyzed.

Formulation of the Problem

Consider the flow of blood in an artery modeled as a rigid circular tube of radius \bar{R} . The blood is modeled as a Herschel–Bulkley fluid. It is assumed the pulsatile flow in the artery is due to a prescribed periodic pressure gradient along the axis of the artery. The flow is taken to be axially symmetric, laminar and fully developed. The length of the artery is assumed to be large enough when compared to its diameter so that entrance, end and special wall effects can be neglected. We use the cylindrical polar coordinates $(\bar{r}, \bar{\phi}, \bar{z})$, where \bar{r} and \bar{z} denote the radial and axial coordinates and $\bar{\phi}$ is the azimuthal angle. Fig. 1 shows the geometry of the stenosed artery.

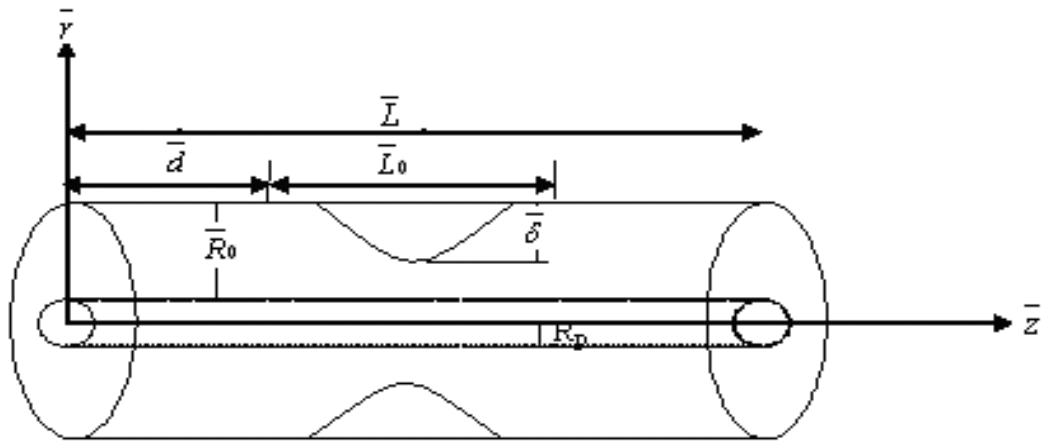


Fig.1. Geometry of stenosed artery

The momentum equations are

$$\bar{\rho} \frac{\partial \bar{u}}{\partial \bar{t}} = -\frac{\partial \bar{p}}{\partial \bar{z}} - \frac{1}{\bar{r}} \frac{\partial}{\partial \bar{r}} (\bar{r} \bar{\tau}) \quad (1)$$

where $\bar{\rho}$ denote the density, \bar{u} the axial velocity, \bar{t} the time, \bar{p} the pressure and $\bar{\tau}$ the shear stress.

The general form of the constitutive equation for Herschel-Bulkley fluid is taken to be.

$$\bar{\mu}_H \left| \frac{\partial \bar{u}}{\partial \bar{r}} \right| = (|\bar{\tau}| - \bar{\tau}_H)^n \quad \text{for} \quad |\bar{\tau}| \geq \bar{\tau}_H \quad (2)$$

$$\frac{\partial \bar{u}}{\partial \bar{r}} = 0 \quad \text{for} \quad |\bar{\tau}| \leq \bar{\tau}_H \quad (3)$$

where $\bar{\tau}_H$ is the yield stress, \bar{u} is the axial velocity, 'n' is the power index and $\bar{\mu}_H$ is the coefficient of the viscosity for Herschel-Bulkley fluid with dimension $(ML^{-1}T^{-2})^n T$.

The relation corresponds to the vanishing of the velocity gradient in region in which the shear stress is less than the yield stress. This implies a plug flow whenever $|\bar{\tau}| \leq |\bar{\tau}_y|$. However, if the shear rates in the fluid is high $|\bar{\tau}| \geq |\bar{\tau}_y|$, then a fluid behaviour is indicated.

The boundary conditions are:

$$\bar{\tau} \text{ is finite at } \bar{r} = 0 \quad \text{and} \quad \bar{u} = 0 \text{ at } \bar{r} = \bar{R}(\bar{z}) \quad (4)$$

Let us consider the pulsatile laminar flow of blood in the z direction through a compliant tube whose radius varies as

$$\frac{\bar{R}(\bar{z})}{\bar{R}_0} = 1 - \bar{\xi} \left[\bar{L}_0^{(m-1)} (\bar{z} - \bar{d}) - (\bar{z} - \bar{d})^m \right], \quad \bar{d} \leq \bar{z} \leq \bar{d} + \bar{L}_0$$

$$= 1, \quad \text{otherwise} \quad (5)$$

Here the parameter $\bar{\xi}$ is expressed as

$$\bar{\xi} = \frac{\bar{\delta}}{\bar{R}_0 \bar{L}_0^m} m^{m/(m-1)}$$

Where $\bar{\delta}$ denote the maximum height of the stenosis at $\bar{z} = \bar{d} + \frac{\bar{L}_0}{m^{m/(m-1)}}$ such that $\frac{\bar{\delta}}{\bar{R}_0} \ll 1$. $\bar{R}(\bar{z})$ and \bar{R}_0 are the radius of artery with and without stenosis respectively.

Method of solution

Let \bar{q}_0 be the absolute magnitude of the typical pressure gradient. Let

$$\bar{\mu}_0 = \bar{\mu}_H \left(\frac{2}{\bar{q}_0 \bar{R}_0} \right)^{n-1} \quad (6)$$

The dimension of the $\bar{\mu}_0$ is the same as the dimension of Newtonian fluid's velocity.

Following non-dimensional variables are introduced:

$$u = \bar{u} / (\bar{q}_0 \bar{R}_0^2 / 2\bar{\mu}), \quad \tau = \bar{\tau} / (\bar{q}_0 \bar{R}_0^2 / 2), \quad r = \frac{\bar{r}}{\bar{R}_0}, \quad z = \frac{\bar{z}}{\bar{R}_0}, \quad \tau = \bar{\tau} \bar{\omega}$$

$$d = \frac{\bar{d}}{\bar{R}_0}, \quad L_0 = \frac{\bar{L}_0}{\bar{R}_0}, \quad \delta = \frac{\bar{\delta}}{\bar{R}_0}, \quad \alpha^2 = \frac{\bar{R}_0^2 \bar{\omega}}{(\bar{\mu}_0 / \bar{\rho})} \quad (7)$$

where ω is the frequency of oscillation of the pulsatile flow and α is called generalized Womersly frequency parameter. The pressure gradient can be written as

$$-\frac{\partial \bar{p}}{\partial \bar{z}}(\bar{z}, \bar{t}) = \bar{q}(\bar{z}) \bar{f}_1(\bar{t}) \quad (8)$$

where $\bar{q}(\bar{z}) = -\frac{\partial \bar{p}}{\partial \bar{z}}(\bar{z}, 0)$, $\bar{f}_1(\bar{t}) = 1 + A' \sin \bar{\omega} \bar{t}$, and A' is the amplitude of the flow. Using the non-dimensional variables eqs. (1), (2) and (3) reduce to

$$\alpha^2 \frac{\partial u}{\partial t} = 2q(z)f(t) + \frac{1}{r} \frac{\partial}{\partial r}(r\tau) \quad (9)$$

where $f(t) = 1 + A' \sin t$, $\theta = \frac{2\bar{\tau}_H}{\bar{q}_0 \bar{R}_0}$, $\alpha^2 = \frac{\bar{R}_0 \bar{\omega} \bar{\rho}}{\bar{\mu}_0}$, $q(z) = \frac{\bar{q}(\bar{z})}{\bar{q}_0}$, $q(z)f(t) > 0$

$$\text{And } \begin{aligned} \frac{\partial u}{\partial r} &= |\tau|^n \left(1 - \frac{n\theta}{|\tau|}\right) & \text{if } |\tau| \geq |\theta| \\ \frac{\partial u}{\partial r} &= 0 & \text{if } |\tau| \leq |\theta| \end{aligned} \quad (10)$$

The boundary conditions in dimensionless form are:

$$\tau \text{ is finite at } r=0 \quad \text{And} \quad u=0 \quad \text{at} \quad r=R(z) \quad (11)$$

The geometry of the stenosis in dimensionless form is given by

$$\begin{aligned} \frac{R(z)}{R_0} &= 1 - \xi \left[L_0^{(m-1)}(z-d) - (z-d)^m \right], & d \leq z \leq d + L_0 \\ &= 1 & \text{otherwise.} \end{aligned} \quad (12)$$

Here the parameter ξ is expressed as

$$\xi = \frac{\delta}{R_0 L_0^m} m^{m/(m-1)}$$

Where δ denote the maximum height of the stenosis at $z = d + \frac{L_0}{m^{m/m-1}}$ such that $\frac{\delta}{R} \leq 1$. $R(z)$ and R_0 is the radius of artery with and without stenosis respectively.

Then the volume flow rate Q is given by

$$Q(t) = 4 \int_0^{R(z)} ru(z, r, t) dr. \quad (13)$$

Solution

The velocity u the shear stress τ , the plug core radius R_p and plug core velocity u_p are assumed to possess the following form:

$$u(z, r, t) = u_0(z, r, t) + \alpha^2 u_1(z, r, t) + \dots \quad (14)$$

$$\tau(z, r, t) = \tau_0(z, r, t) + \alpha^2 \tau_1(z, r, t) + \dots \quad (15)$$

$$R_p(z, t) = R_{0p}(z, t) + \alpha^2 R_{1p}(z, t) + \dots \quad (16)$$

$$u_p(z, t) = u_{0p}(z, t) + \alpha^2 u_{1p}(z, t) + \dots \quad (17)$$

where $\alpha (< 1.0)$ is the Womersly frequency parameter, From Eqs. (10), (15) and (16).

$$\frac{\partial}{\partial r} (r\tau_0) = -2rq(z)f(t) \quad (18)$$

$$\frac{\partial u_0}{\partial t} = \frac{1}{r} \frac{\partial}{\partial r} (r\tau_1). \quad (19)$$

Integrating equation (18) and using the boundary condition of equation (11)

$$\tau_0 = -q(z)f(t)r \quad (20)$$

Substituting Eqs (14) and (15) into equation (10). We obtain

$$-\frac{\partial u_0}{\partial r} = \tau_0^n \left(1 + \frac{n\theta}{\tau_0}\right) \quad (21)$$

$$-\frac{\partial u_1}{\partial r} = \tau_0^{n-2} \tau_1 n \{ \theta(1-n) + \tau_0 \} \quad (22)$$

Substituting Eq (20) in Eq (21) and integrating and using the boundary condition of Eq (11), we obtain

$$u_0 = \{-q(z)f(t)\}^n R^n \left[\frac{R}{n+1} \left\{1 - \left(\frac{r}{R}\right)^{n+1}\right\} + k^2 \left\{1 - \left(\frac{r}{R}\right)^n\right\} \right] \quad (23)$$

where $k^2 = \frac{\theta}{q(z)f(t)}$.

The plug core velocity u_{0p} can be obtained from Eq (24) as

$$u_{0p} = \{-q(z)f(t)\}^n R^n \left[\frac{R}{n+1} \left\{1 - \left(\frac{R_{0p}}{R}\right)^{n+1}\right\} + k^2 \left\{1 - \left(\frac{R_{0p}}{R}\right)^n\right\} \right] \quad (24)$$

Here R_{0p} is the first approximation plug core radius. Neglecting the term α^2 and higher power of α in Eq (17), the expression for R_{0p} can be obtained from Eq (21) as

$$[r]_{|\tau_0|=\theta} = R_{0p} = \frac{\theta}{|-q(z)f(t)|} = k^2 \quad (25)$$

Similarly the solution for τ_1 , u_1 and u_{1p} can be obtained as.

$$\tau_1 = \{-q(z)f(t)\}^n M \left[\frac{1}{2} \left(\frac{R}{n+1} + k^2\right) \left(\frac{r}{R}\right) - \frac{k^2}{(n+2)} \left(\frac{r}{R}\right)^{n+1} - \frac{R}{(n+1)(n+3)} \left(\frac{r}{R}\right)^{n+2} \right] \quad (26)$$

$$u_1 = \{-q(z)f(t)\}^{2n-2} MnR^{n-1} \left[\theta(1-n) \left\{ \frac{1}{2n} \left(\frac{R}{n+1} + k^2\right) \left(1 - \left(\frac{r}{R}\right)^n\right) - \frac{k^2}{2n(n+2)} \left(1 - \left(\frac{r}{R}\right)^{2n}\right) - \frac{R}{(n+1)(n+3)(2n+1)} \left(1 - \left(\frac{r}{R}\right)^{2n+1}\right) \right\} - q(z)f(t)R \left\{ \frac{1}{2(n+1)} \left(\frac{R}{n+1} + k^2\right) \left(1 - \left(\frac{r}{R}\right)^{n+1}\right) - \frac{k^2}{(n+2)(2n+1)} \right\} \right]$$

$$\left. \left(1 - \left(\frac{r}{R} \right)^{2n+1} \right) - \frac{R}{(n+1)(n+3)(2n+1)} \left(1 - \left(\frac{r}{R} \right)^{2n+1} \right) \right\} \quad (27)$$

$$u_{1p} = [u_1] \text{ at } r = R_{0p} \quad (28)$$

where $M = \frac{1}{[f(t)]^n} \frac{d}{dt} [f(t)]^n$, one can easily obtained the expression for velocity distribution from Eqs. (13),(22) and (26). The shear stress on the wall τ_w is given by

$$\tau_w = -q(z)f(t) \left[R + \alpha^2 (-q(z)f(t))^{n-1} M \left\{ \frac{1}{2} \left(\frac{R}{n+1} + k^2 \right) - \frac{k^2}{n+2} - \frac{R}{(n+1)(n+3)} \right\} \right] \quad (29)$$

The volumetric flow rate is given by

$$\begin{aligned} Q(t) = & 4 \left\{ -q(z)f(t) \right\}^n R^n \left[2 \left(\frac{R}{n+1} + k^2 \right) - \frac{R^2}{(n+1)(n+3)} - \frac{k^2 R^2}{n+3} \right] \\ & + \alpha^2 M n \left\{ -q(z)f(t) \right\}^{2(n-1)} R^{n-1} \left[\left\{ \frac{1}{n} \left(\frac{R}{n+1} + k^2 \right) - \frac{k^2}{n(n+2)} \right. \right. \\ & - \frac{2R}{(n+1)(n+2)(2n+1)} - \frac{1}{2n} \left(\frac{R}{n+1} + k^2 \right) \frac{k^2}{n+2} - \frac{R^2 k^2}{4n(n+1)(n+2)} \\ & \left. \left. + \frac{R^3}{(n+1)(n+3)(2n+2)(2n+3)} \right\} - q(z)f(t) R \left\{ \frac{1}{n+1} \left(\frac{R}{n+1} + k^2 \right) \right. \right. \\ & - \frac{2k^2}{(n+1)(2n+1)} - \frac{R}{(n+1)^2(n+3)} - \frac{1}{2(n+1)} \left(\frac{R}{n+1} + k^2 \right) \frac{R^2}{(n+3)} \\ & \left. \left. + \frac{k^2 R^2}{(n+2)(2n+1)(2n+3)} + \frac{R^3}{(n+1)(n+3)(2n+2)(2n+3)} \right\} \right] \quad (30) \end{aligned}$$

From Eq (31) for small $\frac{k}{\sqrt{R}}$ and $\alpha \ll 1$. So neglecting the term α^2 and higher power of α .

$$q(z)f(t) = \left[\frac{Q(t)}{R} \left\{ 8 \left(\frac{R}{n+1} + k^2 \right) - \frac{R^2}{(n+1)(n+3)} - \frac{k^2 R^2}{(n+3)} \right\}^{-1} \right]^{1/3} \quad (31)$$

The resistance to flow λ is defined as

$$\lambda = (p_1 - p_2) f(t) / Q(t) \quad (32)$$

The second approximation plug core radius R_{1p} can be obtained by neglecting the term with α^4 and the higher power of α in Eq (16) in the following manner

The shear stress $|\tau| = (|\tau_0| + \alpha^2 |\tau_1|)$ at $r = R_p$ is given by

$$\left[|\tau_0| + \alpha^2 |\tau_1| \right] = \theta \quad \text{at} \quad r = R_p \quad (33)$$

Using Taylor's series of $|\tau_0|$ and $|\tau_1|$ about R_{0p} and using $|\tau_0(R_{0p})| = \theta$, we get

$$R_{1p} = -|\tau_1(R_{0p})| / q(z)f(t) \quad (34)$$

With the help of Eqs. (16), (25), (26) and (34), R_p can be given by

$$R_p = k^2 + \alpha^2 \{-q(z)f(t)\}^{n-1} M \left[\frac{1}{2} \left(\frac{R}{n+1} + k^2 \right) \frac{k^2}{R} - \frac{k^2}{(n+2)} \left(\frac{k^2}{R} \right)^{n+2} - \frac{R}{(n+1)(n+3)} \left(\frac{k^2}{R} \right)^{n+2} \right] \quad (35)$$

The longitudinal impedance of the artery is given by

$$\Lambda = \frac{q(t)}{Q} \quad (36)$$

Results and Discussions

The change in the flow pattern and the effects of non-Newtonian nature of blood in an artery are studied and the flow is pulsatile. Blood has been modeled as Herschel-Bulkley fluid which has a definite yield stress θ and power index n . The results are analyzed for different values of non-dimensional variables namely the catheter radius ratio k , yield stress $\bar{\tau}_y$, amplitude A' and generalized Womersly frequency parameter α .

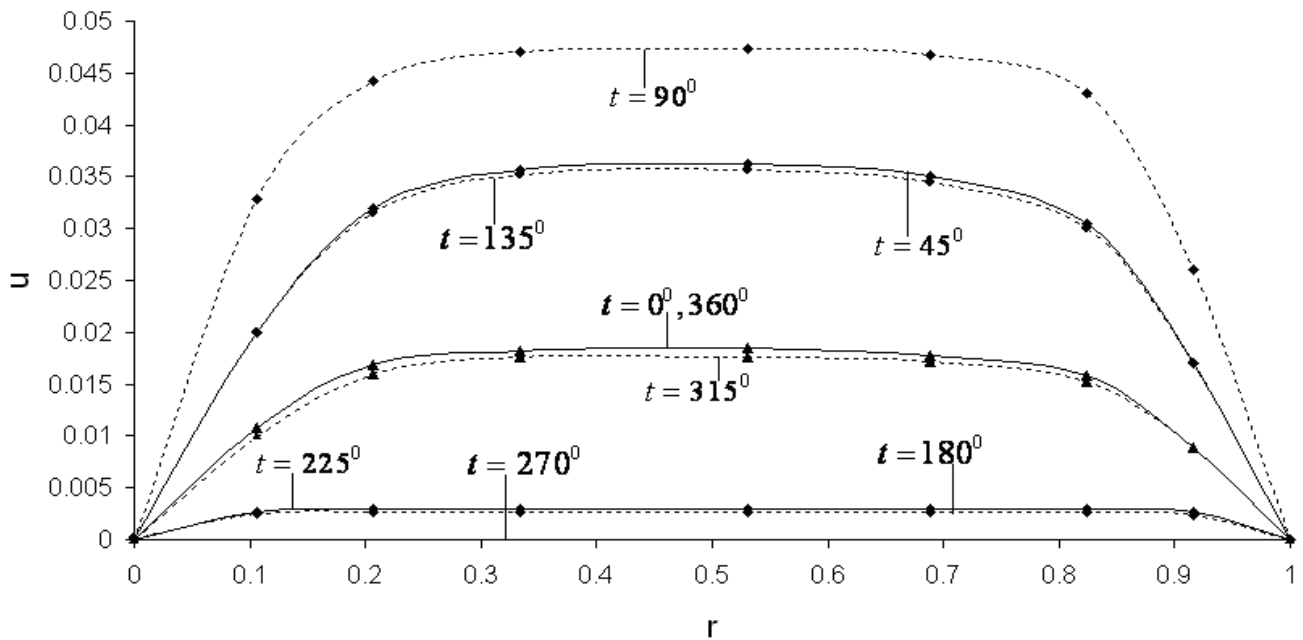


Fig. 2 . Variation of velocity with radial distance during a flow cycle with $\theta = 0.25$, $A' = \alpha = 0.5$ and $n = 0.95$

The variation of velocity with radial distance r during a flow cycle when $\theta = 0.25$, $\alpha = A' = 0.5$ for $n = 0.95$ and 1.05 are shown in Fig. 2. The fluid velocity increases from 0° to 90° and then decreases from 90° to 270° and again increases from 270° to 360° and there is no flow at 270° . As n increases from 0.95 to 1.05 , the velocity decreases slightly for a given A' , θ , α and t .

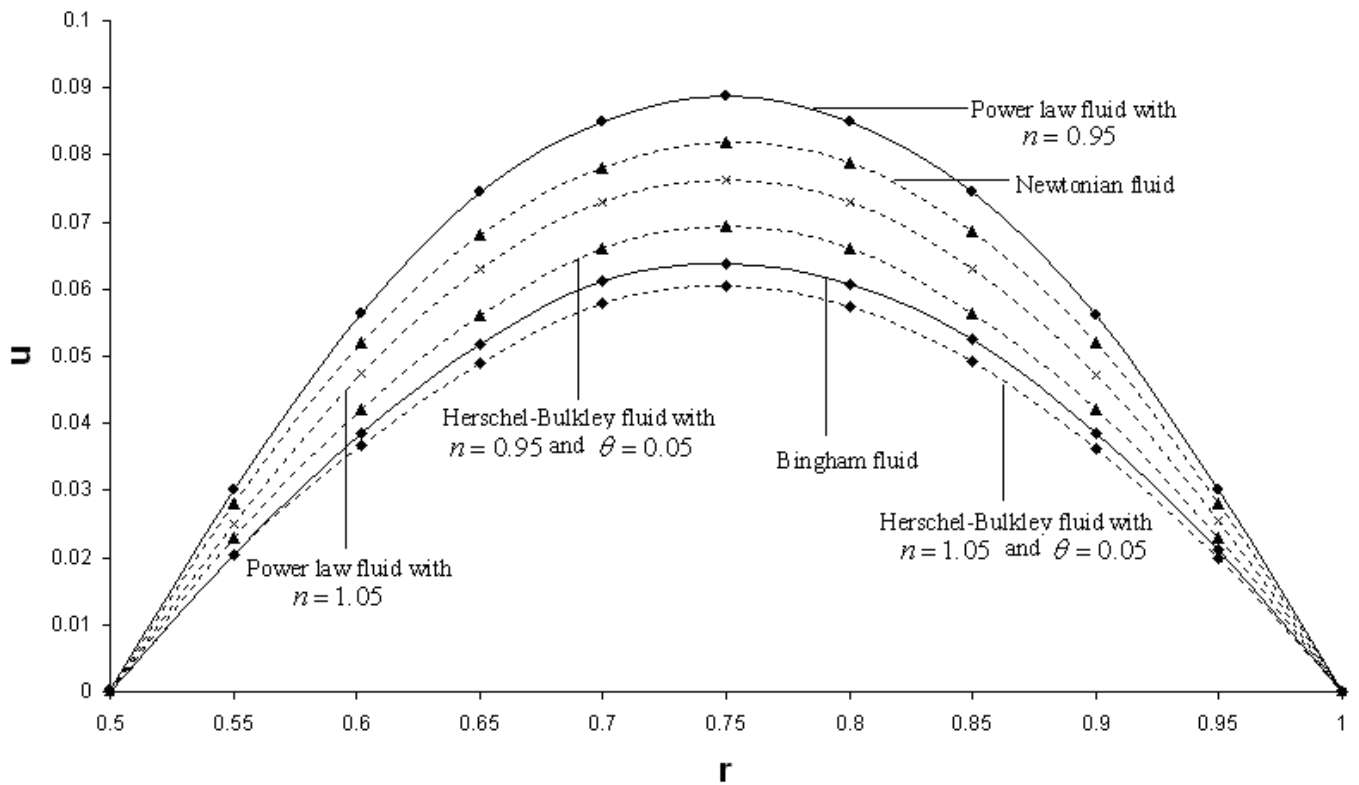


Fig. 3. Variation of velocity with radial distance for different fluids with $A' = \alpha = 0.5$, and $t = 45^\circ$. The variation of velocity with radial direction for different fluids is shown in Fig. 3. We notice that the velocity is greater for power law fluids compared to Herschel-Bulkley fluids for given n and any value of θ . Fig. 3 depicts the effects of the non-Newtonian nature of the fluids on velocity in radial direction.

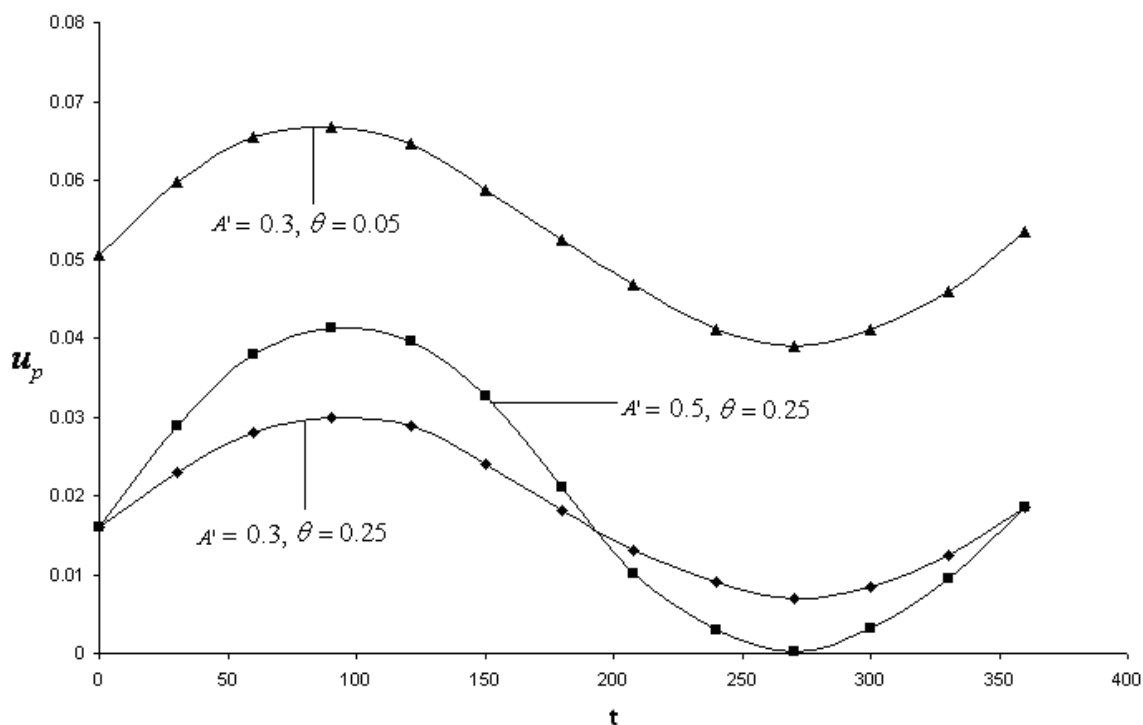


Fig. 4. Variation of plug flow velocity in a flow cycle for different values of A' and θ with $\alpha = 0.5$ and $n = 0.95$

Fig.4 depicts the variation of plug flow velocity in a cycle of oscillation for different values of amplitude A' and yield stress θ with $\alpha = 0.5$ and $n = 0.95$. For a given A' , θ and n , it is clear that the plug flow velocity increases as t increases from 0° to 90° and then decreases from 90° to 270° and again increases from 270° to 360° . The plug flow velocity is maximum at 90° and minimum at 270° . Also it is observed that the plug flow velocity decreases as the yield stress θ increases for a given A' . For a given θ , as the amplitude increases from 0.3 to 0.5, the plug flow velocity increases when t lies between 0° and 180° and it decreases when t lies between 180° and 360° . The same behaviour is observed for $n = 1.05$. It is noticed that the plug flow velocities for Herschel–Bulkley fluid with $n = 0.95$ and $n = 1.05$ are slightly higher than the values for Casson fluid. Fig.4 analyses the effects of yield stress on plug flow velocity during a time cycle.

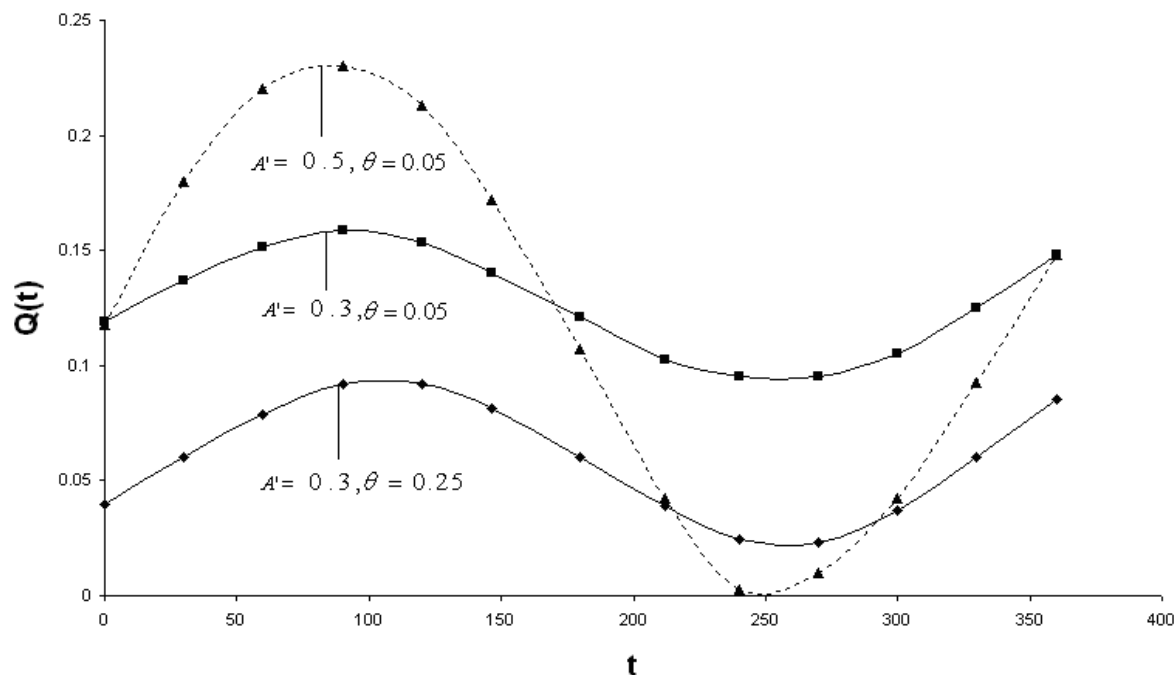


Fig. 5. Variation of flow rate in a cycle of oscillation for different values of A' and θ with $n = 0.95$ and $\alpha = 0.5$.

Fig. 5 depicts the variation of flow rate during a cycle of oscillation for different values of amplitude A' and yield stress θ with $\alpha = 0.5$ for $n = 0.95$. The flow rate increases as t increases from 0° to 90° , decreases when t increases from 90° to 270° and again increases as t increases further from 270° to 360° for fixed values of A' , θ , and α . The flow rate is maximum when $t = 90^\circ$ and minimum when $t = 270^\circ$. This is an obvious result from the velocity distribution. It is observed that the flow rate decreases as the yield stress θ increases for a given value of amplitude A' and for any value t . As the amplitude A' increases, the flow rate increases when t lies between 0° and 180° and it decreases when t lies between 180° and 360° . It is noticed that the flow rate decreases slightly when the power index n increases from 0.95 and 1.05, keeping all the other parameters fixed. Fig. 5 analyses the effects of yield stress on flow rate during a time cycle.

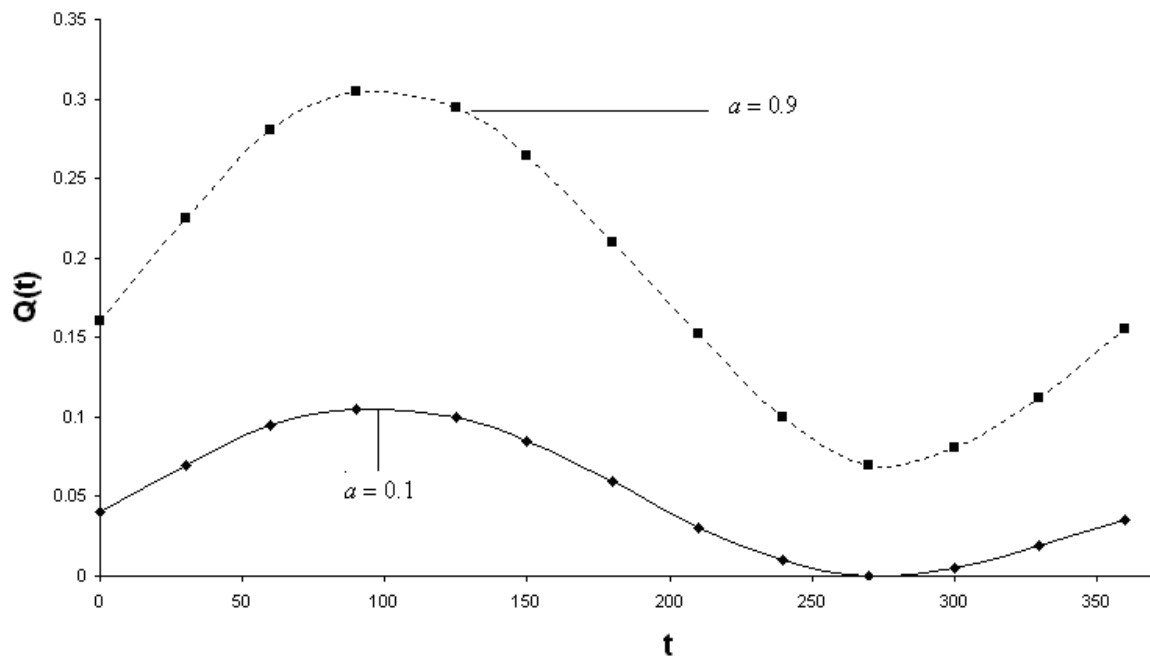


Fig. 6. Variation of flow rate in a cycle of oscillation for different values of α with $n = 0.95$, $A' = 0.5$ and $\theta = 0.5$.

Fig.6 shows the variation of flow rate in a flow cycle for different values of α when $n = 0.95$, $\theta = 0.25$ and $A' = 0.5$. It is observed that the variation of flow rate with increasing α is almost negligible. When the flow rate values for Herschel–Bulkley fluid are compared with that of Casson fluid for $\alpha = A' = 0.5$ and $\theta = 0.05$, the flow rates for Herschel–Bulkley fluid for $n = 0.95$ and 1.05 are almost double than that of Casson fluid for any t . Fig. 6 discusses the effects of the pulsatility of blood flow during a time cycle.

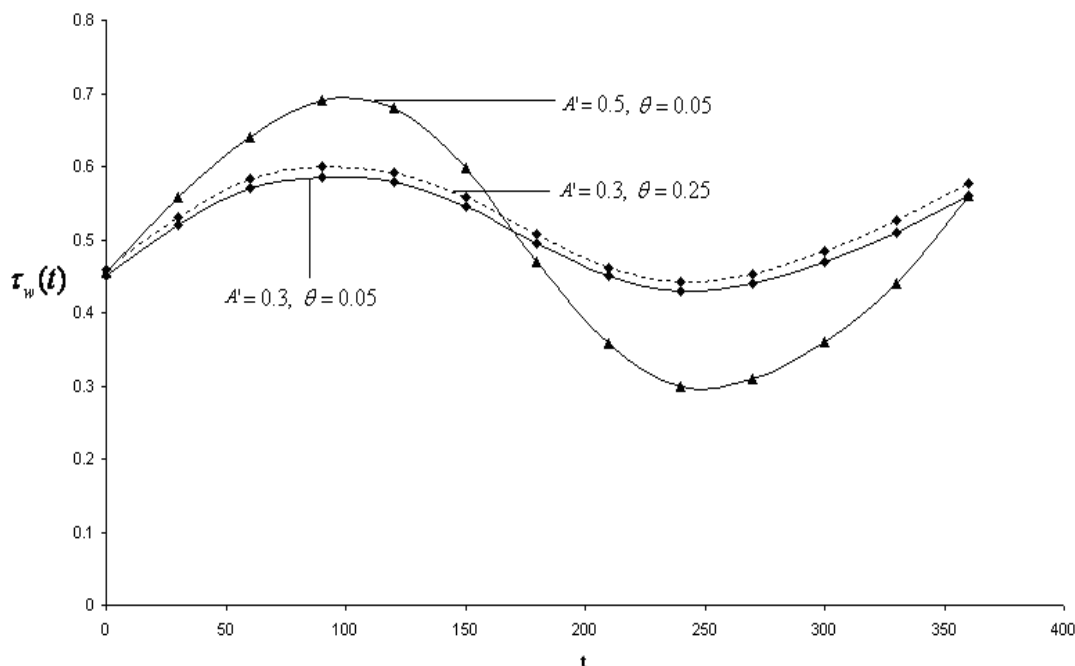


Fig. 7. Variation of wall shear stress in a cycle of oscillation for different values of A' and θ with $n = 0.95$ and $\alpha = 0.5$.

The variation of wall shear stress in a cycle of oscillation for different values of amplitude A' and yield stress θ with $\alpha = 0.5$ for $n = 0.95$ is shown in Fig.7. The wall shear stress increases as t increases from 0° to 90° , decreases as t increases from 90° to 270° and again increases as t increases further from 270° to 360° when A' , α , θ and n are fixed. The maximum wall shear stress is attained at $t = 90^\circ$ and the minimum wall shear stress is attained at $t = 270^\circ$. For the given values of n , t , and A' , the wall shear stress increases as the yield stress increases. It is noticed that as the amplitude A' increases, the wall shear stress increases when t lies between 0° and 180° and it decreases as t lies between 180° and 360° for the given values of α , θ and n . It was observed that for any t and fixed values of α , θ and A' , the wall shear stress increases slightly for $n = 1.05$ compared to that of $n = 0.95$. Fig. 7 shows the variation of wall shear stress with amplitude A' and yield stress θ during a time cycle.

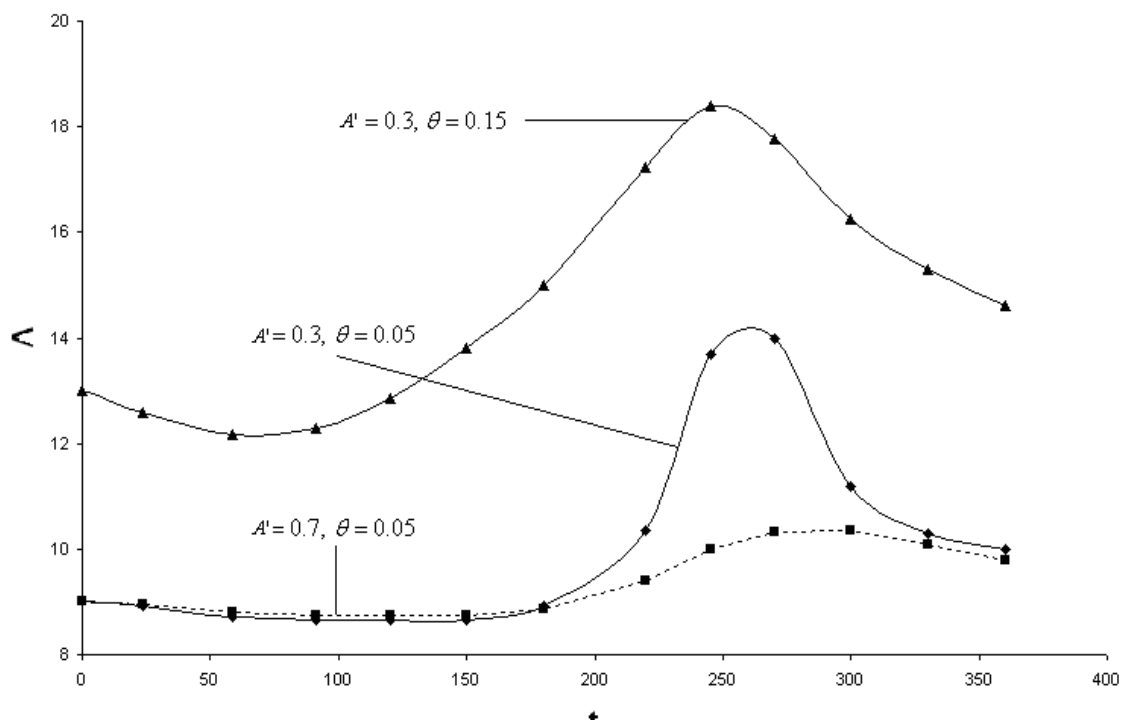


Fig. 8. Variation of longitudinal impedance in a cycle of oscillation for different values of A' and θ with $n = 0.95$ and $\alpha = 0.5$.

Variation of longitudinal impedance during a flow cycle for different values of amplitude A' and yield stress θ with $\alpha = 0.5$ and $n = 0.95$ is depicted in Fig. 8. As seen from Fig. 8, the longitudinal impedance decreases as t increases from 0° to 90° , it increases from 90° to 270° and decreases from 270° to 360° for given values of A' , θ , and α . The longitudinal impedance is minimum at 90° and maximum at 270° . It is clear that the longitudinal impedance increases considerably as the yield stress θ increases from 0.05 to 0.15 for any t and for a given value of A' . For a fixed value of yield stress θ , the longitudinal impedance increases slightly when t lies between 0° and 180° and decreases considerably when t lies between 180° and 360° as the amplitude increases from 0.3 to 0.7 with the given values of α . Fig. 8 depicts the non-Newtonian nature of the fluid on longitudinal impedance.

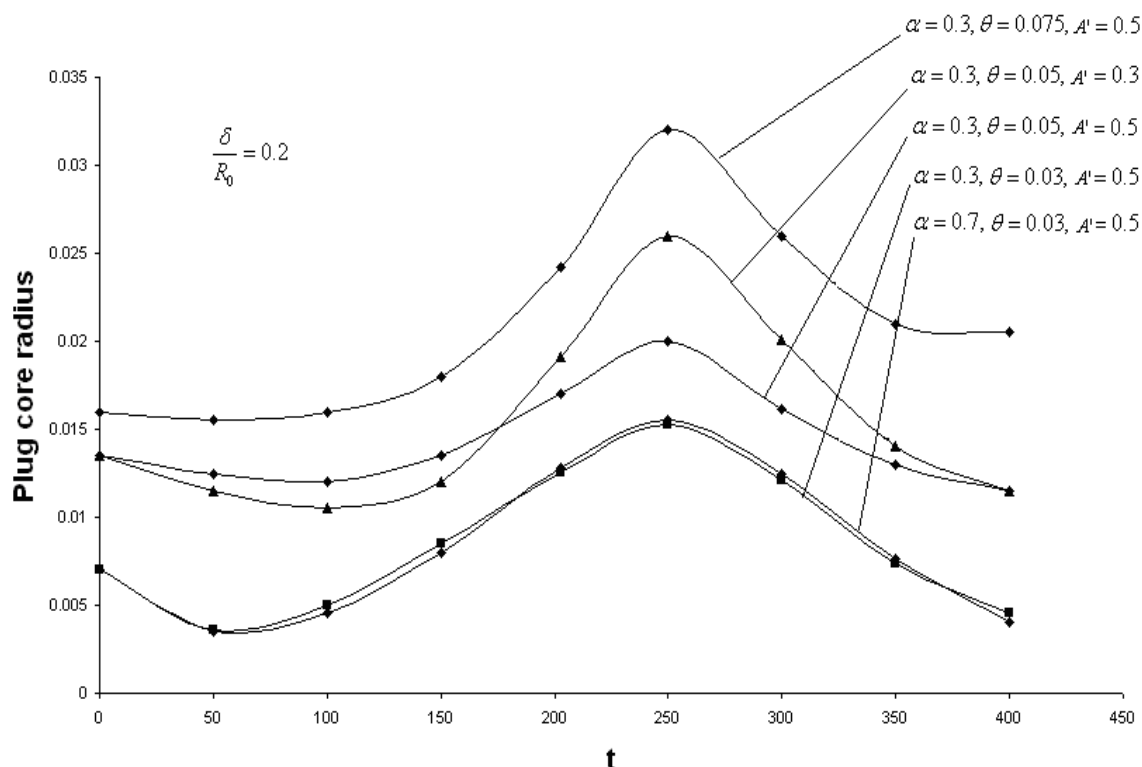


Fig. 9. Variation of plug core radius with time at the centre of Stenosis for different values of A' , θ and α .

Fig. 9 shows the effects of the various parameters ($\alpha, A', t, \theta, \delta$) on the plug core radius. In the time cycle, it starts decreasing as t goes from 0° to 90° and from 270° to 360° and reaches its minimum at $t = 90^\circ$ and starts increasing as t goes from 90° to 270° and reaches its maximum at $t = 270^\circ$. It can be observed that an increase in the yield stress leads to an increase in the plug core radius, whereas its variation with δ is of opposite nature. Also it is seen that the plug core radius changes with pulsatile Reynolds number α and this change is higher for higher values of α . It may be noted that the mean plug core diameter is greater than the steady core diameter.

Conclusion

The present study deals with the pulsatile flow of Herschel–Bulkley fluid through stenosed artery. For the fixed values of n and A' , the width of the plug flow region increases as the yield stress increases. The width of the plug flow region decreases as t increases from 0° to 90° and then increases as t increases from 90° to 270° and decreases when t increases further from 270° to 360° for fixed values of n , A' and θ . During a cycle of oscillation, the maximum flow occurs at $t = 90^\circ$ and the minimum flow occurs at $t = 270^\circ$. As the power index n increases from 0.95 to 1.05, the velocity and flow rate decrease but the wall shear stress and longitudinal impedance increase while all the other parameters are fixed. For the fixed values of the parameters A' , n and α , the velocity and flow rate decrease whereas wall shear stress and longitudinal impedance increase with increasing values of yield stress θ . As the generalized Womersley frequency parameter α increases, the wall shear stress decreases when t lies

between 0° and 90° , and increases when t lies between 90° and 270° and decreases when t lies between 270° and 360° when A' , n and θ are held constant. The variations in velocity, flow rate and longitudinal impedance are negligible due to the variation in generalized Womersley frequency parameter α . For the fixed values of θ with increasing A' , the width of the plug flow region decreases as t lies between 0° and 180° but increases when t lies between 180° and 360° .

References

1. Aroesty, J., and Gross, J.F., (1972), "Pulsatile flow in small vessels – I Casson theory", *Biorheology* Vol. 9, pp. 33–42.
2. Back, L.H., Radbill, J.R., Cho, Y.I., Crawford, D.W., (1986), "Measurement And Prediction Of Flow Through A Replica Segment Of A Mildly Atherosclerotic Coronary artery Of Man". *Journal of Biomechanics*, Vol.19, pp. 1-17.
3. Belardinelli, E., Cavalcanti, S., (1991), "A new non-linear two-dimensional model of blood motion in tapered and elastic vessels", *Comput. Bio. Med.*, Vol. 21, pp 1-13.
4. Chakravarty, S., Sharifuddin, Mandal, P.K., (2004), "Unsteady flow of a two-layer blood stream past a tapered flexible artery under stenotic conditions", *Comput. Methods in Appl. Math.*, Vol. 4(4), pp 391-409.
5. Chaturani, P., Samy, R.P., (1986), "Pulsatile flow of Casson's fluid through stenosed arteries with application to blood flow", *Biorheology*, Vol. 23, pp 499-511.
6. Chaturani. P., and Ponnalagar Samy, R., (1986), "Pulsatile flow of a Casson fluid through stenosed arteries with application to blood flow", *Biorheology* Vol. 23, pp. 499–511
7. Chien, S., (1981), "Hemorheology in clinical medicine, *Rec. Adv. Cardiovascular Dis*". Vol. 2 (Supplement), pp. 21–26.
8. Dash, R.K., Jayaraman. G., and Metha, K.N., (1996), "Estimation of increased flow resistance in a narrow catheterized artery – A theoretical model", *J. Biomech.* Vol. 29, pp. 917–930.
9. Despande, M.D., Giddens, D.P., Mabon, R.F., 1976, "Steady Laminar Flow Through Modelled Vascular Stenoses". *Journal of Biomechanics*, Vol.9, pp. 165-174.
10. Gijssen, F.J.H., van de Vosse, F.N., Janssen, J.D., (1999), "The influence of the non-Newtonian properties of blood on the flow in large arteries: Steady flow in a carotid bifurcation model", *J. Biomech.*, Vol. 32, pp 601-608.
11. Haldar, K., (1987), "Oscillatory flow of blood in a stenosed artery", *Bull. Math. Bio.*, Vol. 49(3), pp 279-287.
12. Imeada, K., Goodman, F.O., (1980), "Analysis of non-linear pulsatile blood flow in arteries", *J. Biomech.*, Vol. 13, pp 1007-1022.
13. Johnston, B., Johnston, P.R., Corney, S., Kilpatrick, D., (2004), "Non-Newtonian blood flow in human right coronary arteries: Steady state simulations", *J. Biomech.*, Vol. 37, pp 709-720.
14. Leuprecht, A., Perktold, K., (2001), "Computer simulation of non-Newtonian effects on blood flows in large arteries", *Computer Methods in Biomech. & Biomedical Engg.*, Vol. 4, pp 149-163.

15. Mishra, J.C., Patra, M.K., Mishra, S.C., (1993), "A non-Newtonian fluid model for blood flow through arteries under stenotic condition", *J. Biomech.*, Vol. 26, pp 1129-1141.
16. Mishra, J.C., Chakravarty, S., (1986), "Flow in arteries in the presence of stenosis", *J. Biomech.*, Vol.19, pp 907-918.
17. Nakamura, M., Sawada, T., (1990), "Numerical study of the unsteady flow on non-Newtonian fluid", *J. Biomech. Engg, Trans. ASME*, Vol. 112, pp 100-103.
18. Neofytou, P., Drikakis, D., (2003), "Non-Newtonian flow instability in a channel with a sudden expansion", *J. non-Newtonian Fluid Mech.*, Vol. 111, pp 127-150.
19. Ookawara, S., Ogowa, K., (2000), "Flow properties of Newtonian and non-Newtonian fluid downstream of stenosis", *J. Chem. Engg. of Jap.*, Vol. 33, pp 582-590.
20. Pak, B., Young, Y.I., Choi, S.U.S., (1990), "Separation and re-attachment of non-Newtonian fluid flow in a sudden expansion pipe", *J. non-Newtonian Fluid Mech.*, Vol.37, pp 175-199.
21. Scott Blair, G.W., and Spanner, D.C., (1974), "An Introduction to Biorheology, Elsevier Scientific Publishing Company, Amsterdam , pp. 51.
22. Shukla, J.B., Parihar, R.S., Rao, B.R.P., (1980), "Effects of stenosis on non-Newtonian flow of the blood in an artery", *Bull. Math. Bio.*, Vol. 42, pp 283-294.
23. Smedby, O., 1997, "do plaques grow upstream or downstream?" *Arteriosclerosis, Thrombosis and Vascular Biology*, Vol.15, pp. 912-918.
24. Tu, C., Deville, M., Dheur, L., Vanderschuren, L., (1992), "Finite element simulation of pulsatile flow through arterial stenosis", *J. Biomech.*, Vol. 25(10), pp 1141-1152.
25. Tu, C., Deville, M., (1996), "Pulsatile flow in non-Newtonian fluid through arterial stenosis", *J. Biomech.*, Vol. 29, pp 899-908.
26. Tu, C., and Deville, M., (1996), "Pulsatile flow of non-Newtonian fluids through arterial stenosis", *J. Biomech.*, Vol. 29, pp. 899-908.
27. Yeleswarapu, K. K., (1996), "Evaluation of Continuum Models for Characterizing the Constitutive Behavior of Blood", Ph.D. thesis, Deptt. of Mech. Engg., University of Pittsburgh..
28. Zendehebudi, G.R., Moayeri, M.S., (1999), "Comparison of physiological and simple pulsatile flows through stenosed arteries", *J. Biomech.*, Vol.32, pp 959-965.